Bone 55 (2013) 335–346

Contents lists available at SciVerse ScienceDirect

Bone

journal homepage: www.elsevier.com/locate/bone

Original Full Length Article

Diminished response to in vivo mechanical loading in trabecular and not cortical bone in adulthood of female C57Bl/6 mice coincides with a reduction in deformation to load ☆

Bettina M. Willie [a,*], Annette I. Birkhold [a], Hajar Razi [a], Tobias Thiele [a], Marta Aido [a], Bettina Kruck [a], Alexander Schill [a], Sara Checa [a], Russell P. Main [c,d], Georg N. Duda [a,b]

[a] Julius Wolff Institut, Charité-Universitätsmedizin Berlin, Germany
[b] Berlin Brandenburg Center for Regenerative Therapies (BCRT), Charité-Universitätsmedizin Berlin, Germany
[c] Department of Basic Medical Sciences, College of Veterinary Medicine, Purdue University, West Lafayette, IN, USA
[d] Weldon School of Biomedical Engineering, Purdue University, West Lafayette, IN, USA

ARTICLE INFO

Article history:
Received 27 October 2012
Revised 3 April 2013
Accepted 26 April 2013
Available online 1 May 2013

Edited by: David Burr

Keywords:
Bone adaptation
Mechanoresponse
Aging
Tibial compression
Mouse

ABSTRACT

Bone loss occurs during adulthood in both women and men and affects trabecular bone more than cortical bone. The mechanism responsible for trabecular bone loss during adulthood remains unexplained, but may be due at least in part to a reduced mechanoresponsiveness. We hypothesized that trabecular and cortical bone would respond anabolically to loading and that the bone response to mechanical loading would be reduced and the onset delayed in adult compared to postpubescent mice. We evaluated the longitudinal adaptive response of trabecular and cortical bone in postpubescent, young (10 week old) and adult (26 week old) female C57Bl/6J mice to axial tibial compression using in vivo microCT (days 0, 5, 10, and 15) and dynamic histomorphometry (day 15). Loading elicited an anabolic response in both trabecular and cortical bone in young and adult mice. As hypothesized, trabecular bone in adult mice exhibited a reduced and delayed response to loading compared to the young mice, apparent in trabecular bone volume fraction and architecture after 10 days. No difference in mechanoresponsiveness of the cortical bone was observed between young and adult mice. Finite element analysis showed that load-induced strain was reduced with age. Our results suggest that trabecular bone loss that occurs in adulthood may in part be due to a reduced mechanoresponsiveness in this tissue and/or a reduction in the induced tissue deformation which occurs during habitual loading. Therapeutic approaches that address the mechanoresponsiveness of the bone tissue may be a promising and alternate strategy to maintain trabecular bone mass during aging.

Introduction

Daily activity and exercise along with genetic, nutritional, and hormonal factors influence bone mass and architecture, allowing for growth and maintenance of the skeleton to resist fracture during habitual loading. Local adaptive responses to mechanical loading have been demonstrated in various cases, specifically in tennis players, who have greater bone density and bone diameter in their playing arm compared to their non-playing arm [1–3] as well as soccer players, who have higher bone mineral density in their lower limbs compared to age and body mass index-matched control individuals [4].

Although bone is able to accommodate changes in loading circumstances during growth, the adaptive capacity seems to diminish with age as shown in human exercise trials [3,5–13] and experimental animal studies [14–26], leading to compromised material and structural properties [27,28]. A negative bone multicellular unit (BMU) imbalance, where the volume of bone resorbed exceeds that which is formed, exists in postmenopausal women and aged men [29,30]. There is evidence that this imbalance and subsequent decline in bone mass is also present in young adulthood in both men and women [31–33] likely due to reduced bone formation [34]. Riggs et al. [31] reported that women experienced 37% and men experienced 42% of their total lifetime trabecular bone loss before the age of 50, compared to 6% and 15%, respectively for cortical bone. While it is likely that the majority of cortical bone loss, observed later in life is primarily due to reductions in sex steroids, the early-onset of substantial trabecular bone loss observed in both sexes remains unexplained, as reductions in sex steroids are not remarkable

☆ All funding sources supporting publication of a work or study: German Federal Ministry of Education and Research (Bundesministerium für Bildung und Forschung; Osteopath grant/TP6) and the German Research Foundation (Deutsche Forschungsgemeinschaft; WI 3761/1-1).

* Corresponding author at: Julius Wolff Institut, Charité — Universitätsmedizin Berlin, Campus Virchow-Klinikum, Institutsgebäude Süd/Südstraße 2, Augustenburger Platz 1, 13353 Berlin, Germany. Fax: +49 30 450 559938.
E-mail addresses: bettina.willie@charite.de (B.M. Willie), annette.birkhold@charite.de (A.I. Birkhold), hajar.razi@charite.de (H. Razi), tobias.thiele@charite.de (T. Thiele), marta.aido@charite.de (M. Aido), bkruck@gmx.net (B. Kruck), alexander.schill@charite.de (A. Schill), sara.checa@charite.de (S. Checa), rmain@purdue.edu (R.P. Main), georg.duda@charite.de (G.N. Duda).

8756-3282/$ – see front matter © 2013 Elsevier Inc. All rights reserved.
http://dx.doi.org/10.1016/j.bone.2013.04.023

in adults. Loss of trabecular bone in adulthood has not only been observed in humans. Glatt et al. [35] demonstrated that trabecular bone volume of C57Bl/6J mice peaked at 6–8 weeks of age and declined steadily thereafter, particularly in the metaphyseal region of long bones, which was more pronounced in females than males. They observed a rapid decrease in trabecular number between 2 and 6 months of age, with a more gradual decline thereafter, whereas trabecular thickness increased slowly over the mouse's lifespan. In contrast, cortical thickness increased markedly from 1 to 3 months of age and was maintained or slightly decreased thereafter [35].

Either the skeleton's ability to form new bone declines with increasing age [34,36] or the appropriate stimulus required to form new bone in an aged skeleton is not perceived. The underlying mechanism(s) responsible for this alteration are largely unknown. Although reduced skeletal loading [37,38] and decreased muscle mass [39–41] may contribute to age-related bone loss, experimental and clinical data suggests that they are not the primary factors [37]. Previous studies have suggested that reduced mechanosensitivity of the bone or a reduced capacity of the bone to respond to loading may at least in part contribute to the pathogenesis of age-related bone mineral loss [42]. Some studies indicate that aging alters levels of circulating hormones [43–47], lowers basal cell function [48–53], decreases the populations of osteoblasts, lining cells, and osteocytes [54,55], and thus degrades the overall mechanoresponsiveness of bone tissue [21,23,38,56]. Additionally, increased bone stiffness with aging particularly in perilacunar tissue could potentially attenuate the strain signal that the osteocyte senses, thereby contributing to bone loss [57–59].

A number of exercise trials demonstrate that physical stimuli that enhance osteogenesis in young people aren't as effective in older individuals. High impact and high velocity exercise increase trabecular bone mass in prepubescent girls [5] and premenopausal women [6–9] as well as maintain bone mass or lead to modest increases in postmenopausal women [10–12]. Premenopausal women had a 2.8% increase in bone mineral density (BMD) in response to 5 months of the same high impact exercise compared to no change in BMD in postmenopausal women [13]. Although a reduced response to loading is clearly shown after menopause, virtually no studies have directly compared the mechanoresponsiveness of teenage or young girls to adult premenopausal women. Kontulaninen et al. [3] showed a reduced response in cortical bone in the playing arms ~44 year old women compared to ~27 year old women, but attributed these differences to when the women first started playing tennis or squash, prior to or after menarche.

Although several experimental studies have examined changes in the responsiveness of cortical bone with aging [14–23], few have addressed trabecular bone [24–26,60]. Most of these studies focused on comparing mechanoresponsiveness in elderly (~78 wk old) versus adult (~26 wk old) rodents, or were exercise-based studies that introduce systemic effects and do not allow for strict control of the loading parameters. Two studies that examined tibial compressive loading in young and adult female C57Bl/6 mice reported contrary results concerning the effect of loading on trabecular bone formation, with one reporting increases in 26 week old mice [26] and the other decreases in 20 week old mice [25]. The mechanical strains induced in the trabecular region were not determined in the latter study, therefore it remains unknown whether these differences in the induced bone response were due to differences in the mechanical stimulation of the bone in the proximal tibia. In addition, both studies were limited to the analysis of the bone response at one specific time point following the 2 wk loading period. Since bone remodeling is a highly dynamical process, investigations of bone adaptation at several time points might help us to better understand the onset and the dynamics of the bone response to mechanical signals. In this study, we aimed to investigate the longitudinal adaptive response of trabecular and cortical bone of postpubescent, young (10 week old) and adult (26 week old) female C57Bl/6J mice to two weeks of controlled noninvasive tibial compression. We assessed the trabecular and cortical bone response to loading using in vivo microCT (days 0, 5, 10, and 15) and both static and dynamic histomorphometry at day 15. We hypothesized that trabecular and cortical bone would respond anabolically to loading and that the bone response to mechanical loading at both ages would be reduced and the onset delayed in adult compared to postpubescent mice.

Materials and Methods

Animals

Fifty-two female C57Bl/6J mice (Jackson Laboratories, Sulzfeld, Germany) were received and acclimatized in our animal facility. Mice were housed 3–5 per cage with ad libitum access to food and water. One mouse died during the acclimation phase, prior to the onset of the study and one mouse died at day 5, while under anesthesia for in vivo microCT analysis, otherwise all mice tolerated the experimental procedure well. All animal experiments were carried out according to the policies and procedures approved by the local legal research animal welfare representative (LAGeSo Berlin, G0333/09).

In vivo load–strain calibration

The relationship between applied compression and bone tissue deformation for the right and left tibia was established for young, postpubescent (10 week old) and adult (26 week old) female mice in vivo ($n = 7$/age). This relationship was used to determine the applied load that engendered $+1200$ με at the medial midshaft of the tibia [25,61]. The strain level of approximately $+1200$ microstrain was chosen because it has been shown to elicit an osteogenic response in the mouse tibia [24,62], which corresponds to roughly two to three times the strains engendered on the medial tibia during normal walking in the mouse [25,63]. Single element strain gauges (EA-06-015LA-120, Micromeasurements, Wendell, USA) were prepared and attached to the medial surface of the tibial midshaft aligned with the bone's long axis [64,65]. While mice were anesthetized, a range of dynamic compressive loads (peak loads ranging from -2 to -12 N) were applied between the flexed knee and ankle using an in vivo loading device (Testbench ElectroForce LM1, Bose, Framingham, USA) and load and strain measurements recorded simultaneously using WinTest software (Fig. 1). No tibial fractures occurred within this load range. The slopes of the load–strain regressions [64] were not significantly different between the 10 week old mice (-0.0090 ± 0.0024 N/με) and 26 week old mice (-0.0089 ± 0.0006 N/με) therefore, in our subsequent studies a load magnitude of -11 N was used to induce $+1200$ με in both age groups.

In vivo mechanical loading

The left tibiae of 10 week old and 26 week old female C57Bl/6J mice underwent either in vivo cyclic compressive ($n = 11$/age) or sham loading ($n = 8$/age) (Fig. 1). Loading parameters included: 216 cycles applied daily at 4 Hz (mean mouse locomotory stride frequency) [66], 5 days/week (M–F), for 2 weeks, delivering -11 N peak loads. The triangle waveform included 0.15 s symmetric active loading/unloading, with a constant strain rate of 0.016 ε/s maintained during both the loading and unloading ramp of the waveform in mice of both ages; the strain rate was similar to other loading studies [26,67,68]. The waveform also included a 0.1 s rest phase (-1 N) between load cycles and a 5 s rest inserted between every four cycles. The rest insert has been shown to increase the anabolic response [22], and also accomplishes a reduced number of load cycles in our model, while maintaining the total loading period at approximately 5 min. The right tibia served as an internal control. Sham loading consisted of placing the left leg in the loading device and applying a

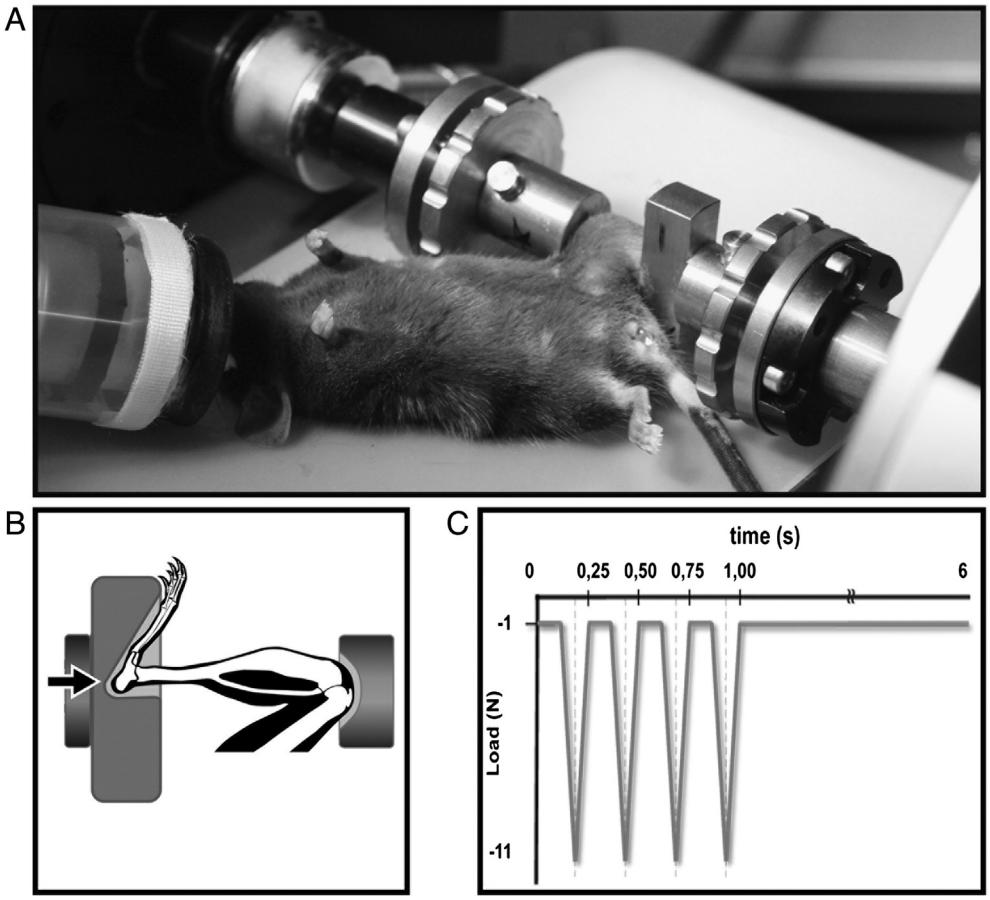

Fig. 1. (A) Photograph of a 10 week old mouse undergoing in vivo loading of the left tibia. (B) Diagram of the mouse hindlimb positioned within the loading device and direction of loading (arrows). (C) Schematic of 6 s of the loading signal, which was repeated 54 times for approximately 5 min each day. Peak-to-peak loading at −11 N resulted in a measured strain of approximately 1200 microstrain at the tibial medial mid-shaft of both aged mice. FE models indicated minimum principal strains of −2410 με and −1695 με (cortical) and −1387 με and −950 με (trabecular) for 10 and 26 week old mice, respectively.

−1 N static preload for the same time duration as those experiencing dynamic loading, approximately 5 min. Mice were sacrificed on day 15, three days after the last loading session, while under anesthesia (ketamine 60 mg/kg and medetomidine 0.3 mg/kg) through an overdose of potassium chloride. After dissection, tibial bone length was measured to be the following: 10 week old loaded mice (single radiated loaded tibia 16.6 ± 0.1 mm, control tibia 16.6 ± 0.1 mm; multiple radiated loaded tibia 16.8 ± 0.5 mm, control tibia 17.0 ± 0.5 mm), 10 week old sham loaded mice (single radiated loaded tibia 16.8 ± 0.3 mm, control tibia 16.7 ± 0.3 mm; multiple radiated loaded tibia 18.0 ± 0.1 mm, control tibia 18.0 ± 0.1 mm), 26 week old loaded mice (single radiated loaded limb: 17.9 ± 0.2 mm, control tibia: 18.1 ± 0.2 mm: multiple radiated loaded tibia 18.1 ± 0.3 mm, control tibia 17.9 ± 0.2 mm), and 26 week old sham loaded mice (single radiated loaded tibia: 17.9 ± 0.1 mm, control tibia: 17.9 ± 0.1 mm: multiple radiated loaded tibia: 18.6 ± 0.3 mm, control tibia: 18.7 ± 0.3 mm). Although mice were randomly assigned to be either sham loaded or loaded, the tibial length of 10 week old sham loaded mice was greater than that of 10 week old dynamically loaded mice. Weight was measured daily throughout the experiment; there was no significant difference in start or end weight between sham loaded or loaded mice.

Micro-computed tomography of trabecular and cortical bone compartments

Longitudinal in vivo microcomputed tomography (microCT) at an isotropic voxel size of 10.5 μm (vivaCT 40, Scanco Medical, Brüttisellen, Switzerland; 55 kVp, 145 μA, 600 ms integration time, no frame averaging) was performed at days 0, 5, 10, and 15 to assess trabecular and cortical bone in the paired tibiae of the 10 and 26 week old loaded (n = 7/age) and sham loaded (n = 4/age) mice. Additional mice were loaded (n = 4/age) or sham loaded (n = 4/age) for two weeks and imaged only at day 15. At days 0, 5, and 10 this latter group of mice underwent the same anesthesia protocol, but were not imaged by microCT in order to determine the influence of repeated radiation exposure on cortical and cancellous bone mass. For each tibia, a trabecular and cortical bone volume of interest (VOI) was defined. The trabecular VOI included secondary spongiosa in the proximal metaphysis, starting 250 μm below the distal-most point of the growth plate and extending distally 5% of the tibial length. The trabecular bone VOI excluded the cortical shell. A global threshold of 2513 HU (456 mg HA/cc) was used to segment trabecular bone from water and soft tissue. Trabecular bone outcome parameters included: bone volume fraction (BV/TV), trabecular thickness (Tb.Th), average number of trabeculae per unit length (Tb.N), trabecular separation (Tb.Sp), and trabecular volumetric tissue mineral density (Tb.vTMD, mg/cc) as recommended [69]. The second VOI included cortical bone and the marrow cavity, centered at the midpoint of the tibia and extending along the bone's long axis 2.5% of the tibial length. A global threshold of 4446 HU (813 mg HA/cc) was used to segment cortical bone from water and soft tissue. Cortical bone outcome parameters included: principal moments of inertia (Imax, Imin), cortical bone area = cortical volume / (number of slices * slice thickness) (Ct.Ar), total cross-sectional area inside the periosteal envelope (Tt.Ar), cortical area fraction (Ct.Ar/Tt.Ar), cortical thickness (Ct.Th), and cortical volumetric tissue mineral density (Ct.vTMD) as recommended [69].

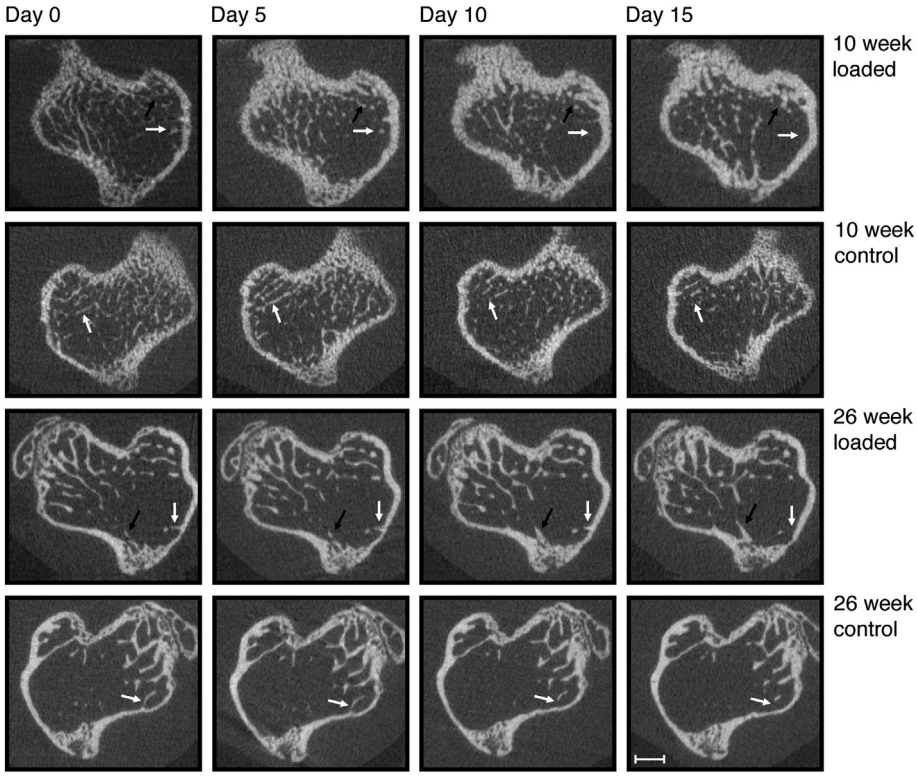

Fig. 2. Cross-sectional microCT images of the trabecular bone from the loaded proximal tibia of 10 and 26 week old mice. For illustrative purposes, images were registered using an established method [92] and are shown here. Each cross-section represents the same area of the bone at days 0, 5, 10, and 15. A greater increase in bone formation over time in response to loading can be observed in 10 week compared to 26 week old mice. Notice that loading maintains a similar amount of bone area in the 26 week old mice over the experimental period due to competing formation and resorption processes. Arrows indicate regions of bone formation (black) and resorption (white). Scale bar: 0.5 mm.

Dynamic histomorphometry

Calcein was administered via intraperitoneal injection, 12 and 3 days before euthanasia. Following dissection of the left and right tibiae from the surrounding soft tissues, tibiae were fixed in 70% ethanol, dehydrated in ascending grades of ethanol to absolute, cleared in xylene, infiltrated, embedded in polymethyl methacrylate, sectioned in the transverse plane at the proximal tibia to analyze trabecular bone and at the mid-shaft to analyze cortical bone (loaded: n = 10/age; sham loaded n = 4/age) in similar regions analyzed by microCT. One, approximately 60 μm thick section from each of the two locations (approximately 200 μm below the growth plate and at mid-shaft) per tibia was adhered to plastic slides, ground and polished to a thickness of approximately 20 μm, and viewed at a magnification of 200× under a mercury lamp microscope (KS400 3.0, Zeiss, Oberkochen, Germany) for evidence of fluorochrome labels. Images were analyzed using a commercial histomorphometric system (Axiovision, Zeiss, Oberkochen, Germany). For trabecular and cortical bone, the single- and double-labeled surface per bone surface (sLS/BS, dLS/BS), mineralizing surface (MS/BS), mineral apposition rate (MAR), and bone-formation rate (BFR/BS), were analyzed as recommended [70]. Single-labeled surface was defined as surface labeled with a single label, while a double-labeled surface was defined as a surface with two labels present. MS/BS was calculated as 0.5x sLS/BS + dLS/BS. When a specimen had no double-labeled surface (dLS/BS = 0), it was coded as "no data" for MAR and BFR/BS [71]. For trabecular bone, MAR was determined by measuring 5 to 10 double labels within one section per tibia and five measurements along the span of each double label. The thickness of newly mineralized bone at the surface of the trabeculae was averaged along the active bone-forming surface, divided by the 9-day labeling interval, and expressed as the MAR in units of microns per day. For cortical bone, the entire endocortical (Ec) and periosteal (Ps) surfaces were analyzed.

Finite element (FE) analysis

MicroCT images of the original strain gauged tibiae were used to develop finite element models of the 10 and 26 week old mice tibiae (n = 1/age). MicroCT images (21 μm resolution) were segmented using the global threshold for trabecular bone (analyzed based on histograms) and converted to finite element meshes using Amira software (Amira, ZIB, Berlin, Germany). The adaptive mesh consisted of tetrahedral elements with average side length of 52 μm (minimum: 5 and maximum: 96 μm, 1.8 million elements). The meshes were then exported to Abaqus (Simulia, Providence, USA) for analysis. Proximal nodes on the tibial plateau were coupled to a reference point [72] where a compressive load of −11 N was applied. The reference point was restrained to axial movement. Surface nodes in the distal part of the bone were restrained from movement in all directions. Lateral radiographs of a cadaveric animal mounted in the loading device were used to correctly align the bone as in the experimental set-up (Fig. 6A). From these images we were able to determine the angle of alignment of the bone with respect to the loading direction. Bone material properties (stiffness) in the fibula and the distal and the proximal tibia were assigned based upon regional differences in tissue mineral density (TMD). Average greyscale values for the fibula and the distal and the proximal tibia (Fig. 6B) were calculated based on the microCT image histograms. Assuming a linear relation between TMD and microCT attenuation values and using the following power relationship between Young's modulus (E) and density (ρ): $E = \text{Constant} \cdot \rho^3$ [73–75]; Young's moduli in the fibula and proximal tibia were calculated as ratios of the distal tibia. Young's

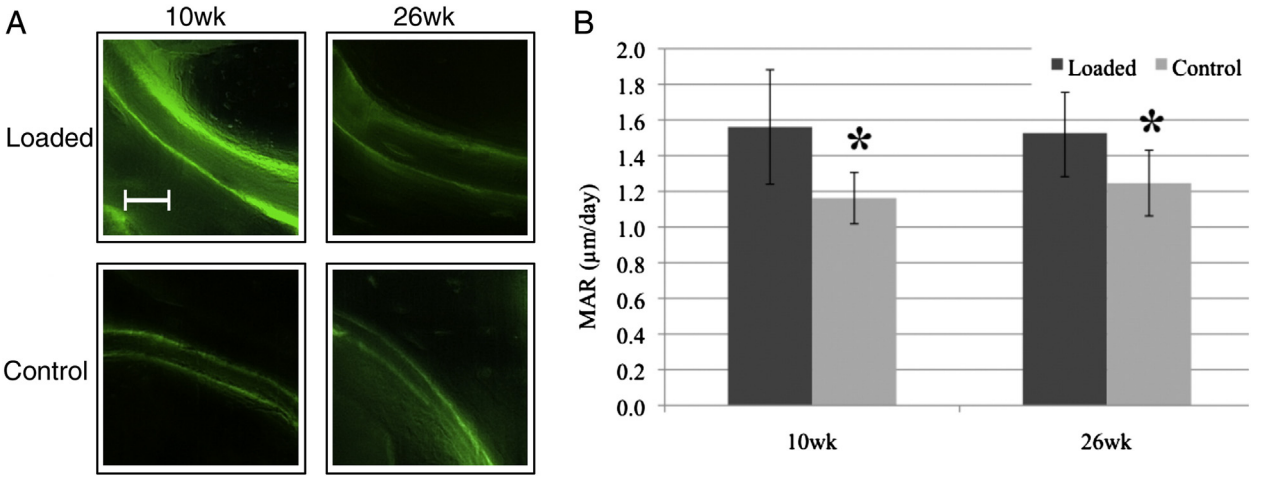

Fig. 3. Effects of loading on trabecular bone formation at the proximal tibia of 10 and 26 week old mice. (A) Double labeling with calcein (administered on days 3 and 12) was assessed in sections from the proximal tibia. (B) Mineral apposition rate (MAR) in trabecular bone from the loaded and nonloaded limb of 10 and 26 week old mice. Data represent the mean ± SD (n = 10/age; *p < 0.05 within-subject effect of loading (loaded, control limbs). Scale bar: (A) 20 μm.

moduli of 16.72 and 15 GPa were implemented for distal tibiae in 26 and 10 wk old mice respectively [59]. The estimated values for the fibula and proximal tibia were 4.93 and 7.64 GPa, respectively for the young mice and 7.85 and 11.6 GPa respectively for the adult mice. Poisson's ratio was set to be 0.35 for all regions of both ages. The corresponding strain gauge value for each bone was calculated by averaging the strain in the direction of the strain gauges at their exact mounting position. This was possible since the same bones were used for strain gauge measurements and the position of the strain gauge was still visible in the scans.

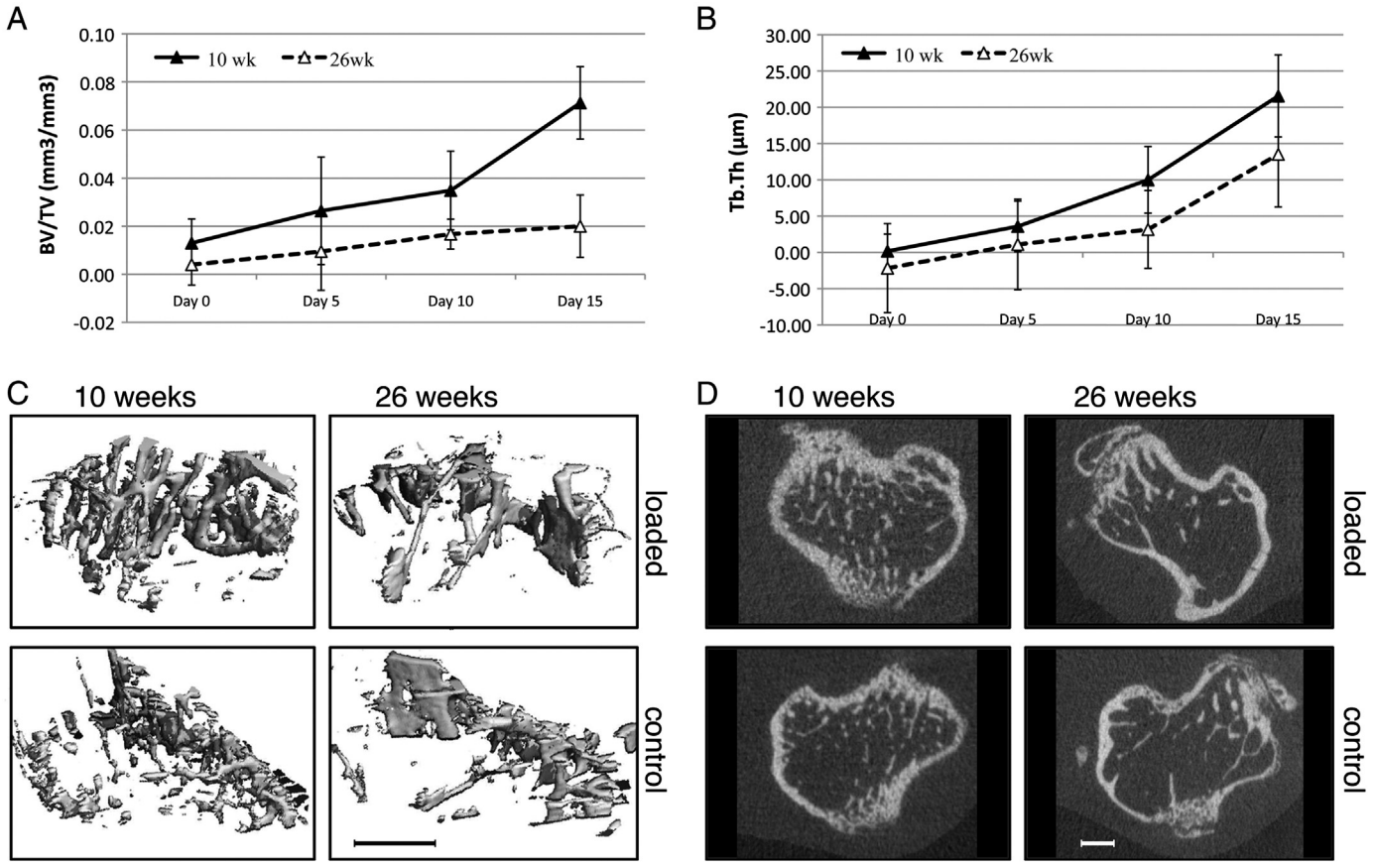

Fig. 4. Relative values (interlimb difference = loaded − control limb), demonstrated that 10 week old mice had a significantly greater trabecular response to loading compared to the 26 week old mice evident in (A) BV/TV and (B) Tb.Th ($p < 0.05$, repeated measures ANOVA). (C) MicroCT 3D and (D) 2D images of the loaded and control limb (proximal tibia) of 10 and 26 week old mice measured at day 15. The images demonstrate a greater area/volume of bone present in the loaded limb of 10 week old compared to 26 week old mice. Notice that the loaded limb of the 26 week old mice has a similar area or volume of bone compared to the control limb of 10 week old mice. The control limb of the 26 week old mice had the least area/volume of bone. Scale bar: (C) and (D) 0.5 mm. Data represent the mean ± SD (n = 11/young mice and n = 10/adult mice).

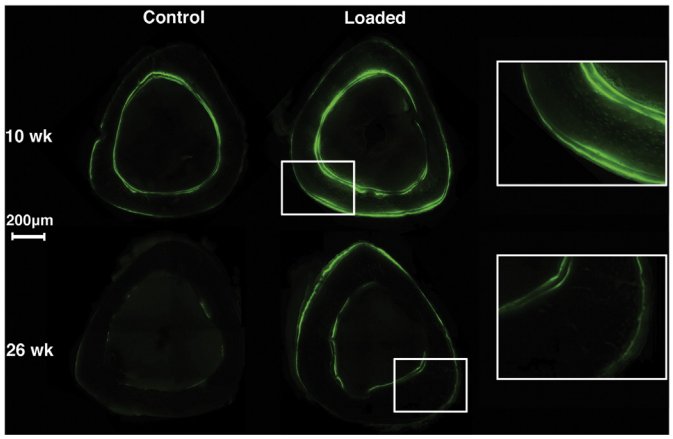

Fig. 5. Fluorescent microscope images of mid-diaphyseal tibial sections from loaded and control tibiae of 10 and 26 week old mice. Samples were collected on day 15 following tibial compression on days 1–5 and days 8–12 and fluorochrome labeling on days 3 and 12. Loading enhanced all cortical bone formation indices measured at day 15 in the 10 and 26 week old mice, except Ec.sLs/BS and Ps.sLs/BS. Although the overall response to loading was similar for the different aged mice, as seen in the microCT parameters, there seemed to be an age-specific regional response to loading with a greater response periosteally in young mice and endosteally in the adult mice. Scale bar: 200 μm.

Statistical analysis

The within-subject effect of loading (loaded, control limbs) and between-subject effects of age (10 week old, 26 week old) as well as interactions between these terms was assessed using a repeated measures ANOVA (SAS 9.3, Cary, USA) for absolute values. A separate repeated measures ANOVA was performed for the sham loaded mice, having a within-subject effect of sham loading (sham loaded, control limb). Relative values (interlimb difference = loaded − control limb) were also analyzed using a repeated measures ANOVA with a within-subject effect of scan day (days 0, 5, 10, 15) and between-subject effects of age (10 week old, 26 week old) as well as interactions between these terms. The onset of the response to loading was assessed using paired t-tests. The effect of radiation exposure was determined using an independent *t*-test. All values are presented as mean ± standard deviation and statistical significance was set at $p < 0.05$.

Results

Age influenced the onset and magnitude of trabecular bone response to loading

When comparing loaded and control limbs we observed that the volume, architecture, and density of trabecular bone was enhanced by loading in mice of both ages over the 15 day experimental period (Table 1). However, the onset of the response was first observed in the 10 week old mice. The loaded limb of the 10 week old mice had a significantly greater BV/TV beginning at day 5 ($p = 0.021$) and significantly greater Tb.Th and Tb.vTMD at day 10 ($p < 0.05$) compared to the control limb (Table 1, Fig. 2). In contrast, the loaded limb of the 26 week old mice had a significantly greater BV/TV starting at day 10 ($p = 0.001$) and Tb.Th ($p < 0.001$), and Tb.vTMD ($p = 0.002$) by day 15 compared to the control limb. However, the loading protocol did not result in trabecular bone gain in the 26 wk old mice, but rather prevented age-related bone loss, as BV/TV levels in the loaded limb remained the same from days 0 to 15, whereas the nonloaded limb and both limbs of the 26 week old sham animals lost bone mass during the 15 day experimental period. In the 10 week old mice, the loaded limb had significantly greater Tb.MAR ($p = 0.001$) and Tb.BFR/BS ($p = 0.050$), while all histomorphometric trabecular bone formation indices were significantly greater in the loaded limb compared to the control limb of 26 week old mice ($p < 0.044$) (Fig. 3, Table 2). Sham loading had no influence on trabecular bone microCT or histomorphometric parameters; with the exception that Tb.sLS/BS was greater in the sham loaded compared to the nonloaded control limbs of 10 week old mice.

When comparing the 10 and 26 week old mice, we observed that at day 0, the 10 week old mice had a significantly lower Tb.Th ($p < 0.001$), Tb.Sp ($p = 0.001$), and Tb.vTMD ($p < 0.001$) than the 26 week old mice. There were no significant differences in the interlimb difference of trabecular bone parameters between the 10 and 26 week old mice at day 0. When analyzing the absolute microCT data for interaction of loading and age (repeated measures ANOVA), the 10 week old mice

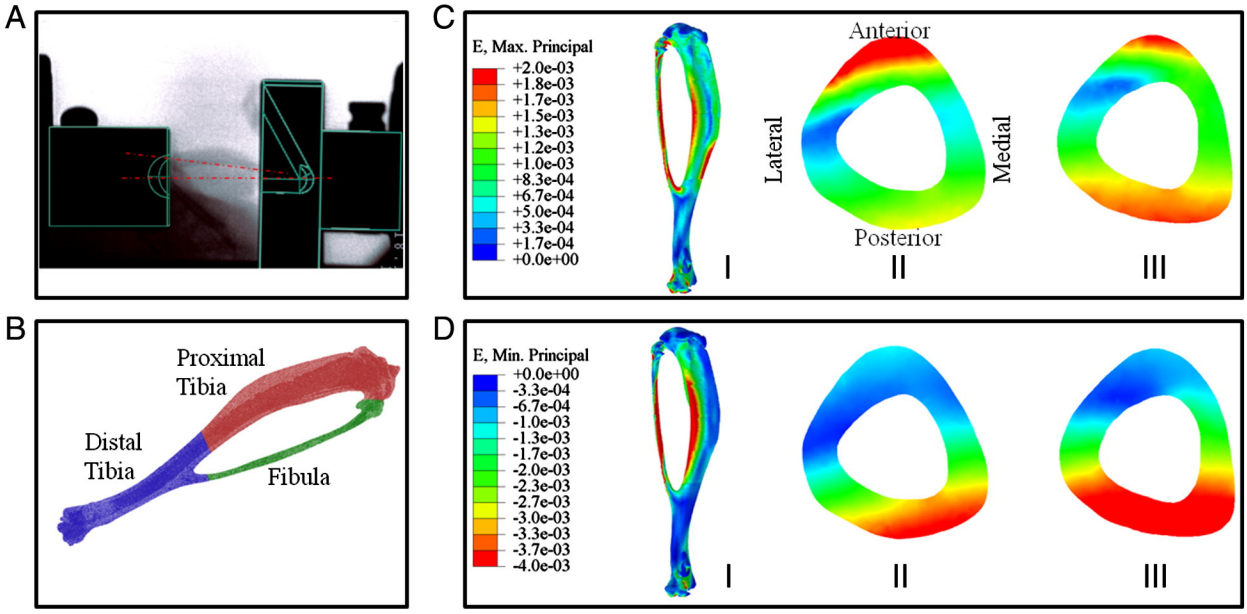

Fig. 6. (A) Radiograph of the bone mounted in the experimental set-up. (B) Three regions (proximal tibia, distal tibia, and fibula) selected for assigning various material property. (C) Principal tensile strain distribution in (I) 26 wk old mouse tibia and cortical transverse sections of (II) 26 and (III) 10 wk old mice. (D) Principal compressive strain distribution in (I) 26 wk old mouse tibia and cortical transverse sections of (II) 26 and (III) 10 wk old mice.

Table 1
Trabecular (Tb) bone parameters of the proximal tibiae, (secondary spongiosa) distal to growth plate, determined by in vivo microCT at days 0, 5, 10 and 15, in mice subjected to axial compression (left tibia was dynamically loaded, right tibia was nonloaded control) and mice subjected to sham loading (left tibia was statically loaded with 1 N, right tibia was nonloaded control) (mean ± SD); for loaded mice groups: [a]within-subject effect of loading (loaded, control limbs), [b]between-subject effects of age (10 week old, 26 week old), and [c]interactions between these terms, $p < 0.05$ assessed using a repeated measures ANOVA.

	10 wk old				26 wk old			
	Loaded mice		Sham loaded mice		Loaded mice		Sham loaded mice	
Outcome	Loaded	Control	Sham loaded	Control	Loaded	Control	Sham loaded	Control
Day 0	(n = 7)	(n = 7)	(n = 4)	(n = 4)	(n = 6)	(n = 6)	(n = 3)	(n = 3)
Tb.BV/TV (mm^3/mm^3)	0.07 ± 0.01	0.06 ± 0.01	0.08 ± 0.00	0.08 ± 0.01	0.06 ± 0.01	0.06 ± 0.01	0.06 ± 0.02	0.05 ± 0.01
Tb.Th (μm)[b]	39 ± 5	39 ± 4	44 ± 2	43 ± 3	54 ± 4	56 ± 6	53 ± 5	52 ± 5
Tb.N (1/mm)	4 ± 0	3 ± 0	4 ± 0	4 ± 0	3 ± 0	3 ± 0	3 ± 0	3 ± 0
Tb.Sp (μm)[b]	285 ± 23	307 ± 21	262 ± 16	283 ± 10	366 ± 22	364 ± 46	376 ± 35	397 ± 45
Tb.vTMD (mg HA/cm^3)[b]	841 ± 36	844 ± 34	903 ± 14	897 ± 13	970 ± 10	972 ± 19	998 ± 18	947 ± 19
Day 5	(n = 7)	(n = 7)	(n = 4)	(n = 4)	(n = 6)	(n = 6)	(n = 3)	(n = 3)
Tb.BV/TV (mm^3/mm^3)[a,b]	0.09 ± 0.03	0.06 ± 0.01	0.08 ± 0.01	0.08 ± 0.02	0.06 ± 0.01	0.05 ± 0.01	0.06 ± 0.01	0.05 ± 0.01
Tb.Th (μm)[b]	43 ± 4	40 ± 3	44 ± 1	46 ± 4	54 ± 4	53 ± 7	51 ± 4	51 ± 5
Tb.N (1/mm)	4 ± 0	4 ± 0	4 ± 0	3 ± 0	3 ± 0	3 ± 0	3 ± 0	2 ± 0
Tb.Sp (μm)[b]	291 ± 39	288 ± 20	267 ± 8	291 ± 20	386 ± 20	394 ± 52	399 ± 54	412 ± 29
Tb.vTMD (mg HA/cm^3)[b]	854 ± 41	861 ± 24	909 ± 38	898 ± 18	973 ± 23	976 ± 24	957 ± 47	968 ± 24
Day 10	(n = 7)	(n = 7)	(n = 4)	(n = 4)	(n = 6)	(n = 6)	(n = 3)	(n = 3)
Tb.BV/TV (mm^3/mm^3)[a,b,c]	0.09 ± 0.02	0.06 ± 0.01	0.07 ± 0.01	0.07 ± 0.00	0.06 ± 0.01	0.04 ± 0.01	0.05 ± 0.01	0.04 ± 0.01
Tb.Th (μm)[a,b,c]	51 ± 4	41 ± 4	44 ± 2	43 ± 5	58 ± 5	55 ± 5	50 ± 8	48 ± 2
Tb.N (1/mm)	3 ± 0	3 ± 0	3 ± 0	3 ± 0	3 ± 0	3 ± 0	2 ± 0	2 ± 0
Tb.Sp (μm)[b]	293 ± 30	324 ± 41	292 ± 24	314 ± 19	404 ± 35	411 ± 65	412 ± 40	438 ± 97
Tb.vTMD (mg HA/cm^3)[a,b]	891 ± 28	865 ± 26	897 ± 24	886 ± 21	989 ± 12	971 ± 27	937 ± 34	956 ± 8
Day 15	(n = 11)	(n = 11)	(n = 8)	(n = 8)	(n = 10)	(n = 10)	(n = 7)	(n = 7)
Tb.BV/TV (mm^3/mm^3)[a,b,c]	0.13 ± 0.02	0.06 ± 0.02	0.07 ± 0.01	0.05 ± 0.01	0.06 ± 0.01	0.04 ± 0.01	0.05 ± 0.01	0.04 ± 0.01
Tb.Th (μm) [a,b,c]	62 ± 5	41 ± 3	44 ± 4	40 ± 3	63 ± 6	50 ± 7	50 ± 5	51 ± 12
Tb.N (1/mm)	4 ± 1	3 ± 1	3 ± 0	3 ± 0	3 ± 0	3 ± 0	3 ± 0	2 ± 0
Tb.Sp (μm)[b,c]	298 ± 51	323 ± 63	295 ± 32	326 ± 39	393 ± 23	390 ± 37	377 ± 47	420 ± 43
Tb.vTMD (mg HA/cm^3)[a,b]	917 ± 23	869 ± 14	909 ± 30	891 ± 27	1004 ± 17	969 ± 23	961 ± 33	918 ± 87

had a greater trabecular bone response to loading compared to the 26 week old mice starting at day 10: BV/TV ($p = 0.027$) and Tb.Th ($p = 0.031$). By day 15, nearly all trabecular microCT parameters showed a significantly greater response to loading in the 10 week old mice compared to the 26 week old mice: BV/TV ($p < 0.001$), Tb.Th ($p = 0.016$), Tb.N ($p = 0.002$), and Tb.Sp ($p = 0.032$). Similar results were observed when analyzing relative values (interlimb difference), with the 10 week old mice showing a significantly greater relative response to loading in BV/TV ($p < 0.001$) and Tb.Th ($p = 0.047$) compared to the 26 week old mice over the experimental period (Fig. 4). An age-related response to loading was not observed in any trabecular histomorphometric parameters. Age-related differences in the response to loading were not observed in any trabecular histomorphometric parameters. As expected there was no significant interaction between age and loading in the sham loaded mice.

Age did not influence the response of cortical bone to loading

Cortical bone mass was enhanced by loading in mice of both ages, with the 10 and 26 week old mice having a similar onset of cortical bone response to loading at day 10 (Table 3). Ct.Ar, Ct.Ar/Tt.Ar, and Ct.Th measured by microCT were significantly greater in the loaded compared to the control limb of 10 week old mice at days 10 and 15 ($p < 0.042$). Similarly, the loaded compared to control limb of 26 week old mice had a significantly greater Ct.Ar/Tt.Ar, and Ct.Th at day 10 and 15 as well as Ct.Ar at day 15 ($p < 0.034$). Loading enhanced all histomorphometric cortical bone formation indices measured at day 15 in the 10 and 26 week old mice, except Ec.sLs/BS and Ps.sLs/BS (Table 4; Fig. 5). Bone formation occurred through lamellar bone formation with no evidence of woven bone present in either age group. Sham loading had no influence on cortical bone microCT parameters or cortical histomorphometric indices.

At day 0, the 10 week old mice had a significantly lower Imax, Imin, Ct.Ar, Tt.Ar, Ct.Ar/Tt.Ar, Ct.Th, Ct.vTMD ($p < 0.002$) than the 26 week old mice measured by microCT. The interlimb difference of cortical bone microCT parameters was similar between the 10 and 26 week old mice observed at day 0. No age-specific response to loading was measured in the cortical microCT parameters over the experimental time period for either the absolute or relative values (interlimb difference). Results from histomorphometric cortical bone formation indices

Table 2
Trabecular bone formation indices from mice subjected to axial tibial compression (left limb was dynamically loaded, right limb was nonloaded control) and mice subjected to sham loading (left limb was statically loaded with 1 N, right limb was nonloaded control) (mean ± SD); for loaded mice groups: [a]within-subject effect of loading (loaded, control limbs), [b]between-subject effects of age (10 week old, 26 week old), and [c]interactions between these terms, $p < 0.05$ assessed using a repeated measures ANOVA.

	10 wk old				26 wk old			
	Loaded mice		Sham loaded mice		Loaded mice		Sham loaded mice	
Outcome	Loaded (n = 10)	Control (n = 10)	Sham loaded (n = 4)	Control (n = 4)	Loaded (n = 10)	Control (n = 10)	Sham loaded (n = 4)	Control (n = 4)
Tb.sLS/BS (%)[a]	21.2 ± 7.0	25.9 ± 1.5	26.5 ± 5.2	23.8 ± 5.2	21.3 ± 3.1	31.3 ± 4.5	30.9 ± 5.2	31.8 ± 5.0
Tb.dLS/BS (%)[a]	32.0 ± 9.9	21.0 ± 6.4	26.3 ± 2.4	24.5 ± 2.7	30.6 ± 10.4	15.6 ± 6.3	18.0 ± 0.6	18.4 ± 7.8
Tb.MS/BS (%)[a]	42.6 ± 12.8	33.9 ± 6.4	39.6 ± 0.2	36.4 ± 5.3	41.3 ± 9.9	31.3 ± 7.5	33.5 ± 2.0	34.4 ± 8.5
Tb.MAR (μm/day)[a]	1.59 ± 0.33	1.16 ± 0.14	0.97 ± 0.12	1.21 ± 0.10	1.53 ± 0.24	1.25 ± 0.18	1.01 ± 0.15	0.91 ± 0.10
Tb.BFR/BS (μm/day)[a]	0.77 ± 0.32	0.40 ± 0.12	0.18 ± 0.25	0.44 ± 0.03	0.64 ± 0.25	0.34 ± 0.17	0.34 ± 0.07	0.32 ± 0.10

Table 3
Cortical (Ct) bone parameters of the mid-tibial diaphysis, determined by in vivo microCT at days 0, 5, 10 and 15, in mice subjected to axial compression (left tibia was dynamically loaded, right tibia was nonloaded control) and mice subjected to sham loading (left tibia was statically loaded with 1N, right tibia was nonloaded control) (mean ± SD); for loaded mice groups: [a]within-subject effect of loading (loaded, control limbs), [b]between-subject effects of age (10 week old, 26 week old), and [c]interactions between these terms, $p < 0.05$ assessed using a repeated measures ANOVA.

	10 wk old				26 wk old			
	Loaded mice		Sham loaded mice		Loaded mice		Sham loaded mice	
Outcome	Loaded	Control	Sham Loaded	Control	Loaded	Control	Sham Loaded	Control
Day 0	(n = 7)	(n = 7)	(n = 4)	(n = 4)	(n = 6)	(n = 6)	(n = 3)	(n = 3)
Imax (mm^4)[b]	0.07 ± 0.01	0.06 ± 0.01	0.07 ± 0.02	0.08 ± 0.00	0.09 ± 0.02	0.10 ± 0.01	0.08 ± 0.01	0.11 ± 0.00
Imin (mm^4)[b]	0.05 ± 0.01	0.04 ± 0.01	0.05 ± 0.01	0.06 ± 0.00	0.06 ± 0.01	0.07 ± 0.00	0.06 ± 0.00	0.07 ± 0.00
Ct.Ar (mm^2)[b]	0.46 ± 0.03	0.46 ± 0.04	0.51 ± 0.04	0.54 ± 0.01	0.59 ± 0.04	0.62 ± 0.02	0.60 ± 0.02	0.64 ± 0.02
Tt.Ar (mm^2)[b]	1.07 ± 0.07	1.03 ± 0.07	1.06 ± 0.09	1.12 ± 0.04	1.16 ± 0.07	1.19 ± 0.05	1.11 ± 0.05	1.24 ± 0.01
Ct.Ar/Tt.Ar (mm^2/mm^2)[b]	0.43 ± 0.02	0.45 ± 0.02	0.48 ± 0.01	0.48 ± 0.01	0.51 ± 0.02	0.52 ± 0.01	0.54 ± 0.02	0.52 ± 0.02
Ct.Th (mm)[b]	0.14 ± 0.01	0.15 ± 0.01	0.16 ± 0.00	0.17 ± 0.00	0.18 ± 0.01	0.19 ± 0.01	0.20 ± 0.01	0.19 ± 0.01
Ct.vTMD (mg HA/cm^3)[b]	1210 ± 13	1236 ± 34	1281 ± 12	1304 ± 9	1337 ± 11	1359 ± 26	1361 ± 7	1372 ± 3
Day 5	(n = 7)	(n = 7)	(n = 4)	(n = 4)	(n = 6)	(n = 6)	(n = 3)	(n = 3)
Imax (mm^4)[b]	0.08 ± 0.01	0.08 ± 0.01	0.10 ± 0.02	0.09 ± 0.01	0.11 ± 0.02	0.11 ± 0.04	0.09 ± 0.00	0.10 ± 0.02
Imin (mm^4)[b]	0.06 ± 0.00	0.05 ± 0.01	0.05 ± 0.01	0.06 ± 0.01	0.07 ± 0.01	0.07 ± 0.01	0.07 ± 0.00	0.06 ± 0.00
Ct.Ar (mm^2)[b]	0.50 ± 0.03	0.49 ± 0.03	0.54 ± 0.03	0.56 ± 0.02	0.61 ± 0.03	0.61 ± 0.04	0.61 ± 0.01	0.62 ± 0.02
Tt.Ar (mm^2)[b]	1.13 ± 0.05	1.11 ± 0.07	1.16 ± 0.09	1.16 ± 0.06	1.22 ± 0.07	1.23 ± 0.09	1.17 ± 0.01	1.18 ± 0.08
Ct.Ar/Tt.Ar (mm^2/mm^2)[b]	0.44 ± 0.02	0.44 ± 0.02	0.47 ± 0.01	0.49 ± 0.01	0.50 ± 0.02	0.50 ± 0.02	0.52 ± 0.02	0.53 ± 0.02
Ct.Th (mm)[b]	0.15 ± 0.01	0.15 ± 0.01	0.16 ± 0.00	0.17 ± 0.00	0.18 ± 0.01	0.18 ± 0.01	0.19 ± 0.01	0.20 ± 0.01
Ct.vTMD (mg HA/cm^3)[b]	1224 ± 21	1233 ± 31	1241 ± 40	1333 ± 8	1315 ± 26	1320 ± 42	1368 ± 3	1383 ± 14
Day 10	(n = 7)	(n = 7)	(n = 4)	(n = 4)	(n = 6)	(n = 6)	(n = 3)	(n = 3)
Imax (mm^4)[b]	0.07 ± 0.02	0.07 ± 0.01	0.07 ± 0.02	0.09 ± 0.02	0.09 ± 0.01	0.09 ± 0.02	0.11 ± 0.05	0.12 ± 0.00
Imin (mm^4)[b]	0.05 ± 0.01	0.05 ± 0.00	0.05 ± 0.01	0.06 ± 0.01	0.06 ± 0.00	0.06 ± 0.01	0.07 ± 0.01	0.07 ± 0.00
Ct.Ar (mm^2)[b]	0.51 ± 0.03	0.48 ± 0.02	0.52 ± 0.03	0.56 ± 0.03	0.59 ± 0.03	0.58 ± 0.03	0.62 ± 0.07	0.63 ± 0.00
Tt.Ar (mm^2)[b]	1.03 ± 0.12	1.05 ± 0.05	1.04 ± 0.11	1.15 ± 0.10	1.14 ± 0.03	1.17 ± 0.08	1.22 ± 0.16	1.27 ± 0.02
Ct.Ar/Tt.Ar (mm^2/mm^2)[a,b]	0.50 ± 0.03	0.46 ± 0.01	0.50 ± 0.03	0.48 ± 0.02	0.52 ± 0.03	0.50 ± 0.03	0.51 ± 0.01	0.49 ± 0.01
Ct.Th (mm)[a,b]	0.17 ± 0.01	0.16 ± 0.00	0.17 ± 0.01	0.17 ± 0.00	0.19 ± 0.01	0.18 ± 0.01	0.18 ± 0.00	0.18 ± 0.01
Ct.vTMD (mg HA/cm^3)[b]	1248 ± 27	1242 ± 24	1296 ± 12	1300 ± 8	1346 ± 22	1356 ± 25	1339 ± 35	1386 ± 7
Day 15	(n = 11)	(n = 11)	(n = 8)	(n = 8)	(n = 10)	(n = 10)	(n = 7)	(n = 7)
Imax (mm^4)[b]	0.07 ± 0.02	0.07 ± 0.01	0.07 ± 0.01	0.07 ± 0.02	0.09 ± 0.01	0.08 ± 0.02	0.09 ± 0.02	0.09 ± 0.01
Imin (mm^4)[b]	0.05 ± 0.01	0.05 ± 0.01	0.05 ± 0.01	0.05 ± 0.01	0.06 ± 0.01	0.06 ± 0.01	0.06 ± 0.01	0.06 ± 0.01
Ct.Ar (mm^2)[a,b]	0.54 ± 0.04	0.48 ± 0.04	0.49 ± 0.05	0.50 ± 0.06	0.61 ± 0.02	0.56 ± 0.04	0.58 ± 0.03	0.56 ± 0.04
Tt.Ar (mm^2)[b]	1.02 ± 0.1	1.03 ± 0.1	1.03 ± 0.08	1.06 ± 0.12	1.12 ± 0.07	1.14 ± 0.09	1.15 ± 0.07	1.16 ± 0.07
Ct.Ar/Tt.Ar (mm^2/mm^2)[a]	0.53 ± 0.04	0.47 ± 0.03	0.48 ± 0.03	0.47 ± 0.03	0.54 ± 0.03	0.49 ± 0.02	0.50 ± 0.01	0.48 ± 0.02
Ct.Th (mm)[a,b]	0.18 ± 0.02	0.16 ± 0.01	0.16 ± 0.02	0.16 ± 0.01	0.20 ± 0.01	0.17 ± 0.01	0.18 ± 0.00	0.17 ± 0.01
Ct.vTMD (mg HA/cm^3)[b]	1268 ± 24	1263 ± 29	1283 ± 32	1286 ± 32	1348 ± 12	1331 ± 31	1346 ± 18	1327 ± 25

were more varied (Table 4). Most histomorphometric parameters indicated no change in responsiveness to loading between the two age groups, except two periosteal indices: Ps.MAR ($p = 0.003$) and Ps.BFR/BS ($p = 0.008$) showed a reduced mechanoresponsiveness in 26 week old compared to 10 week old mice. In contrast, two endocortical indices Ec.MS/BS ($p = 0.043$) and Ec.BFR/BS ($p = 0.013$) suggested a reduced mechanoresponsiveness in 10 week old compared to 26 week old mice. As expected, there was no age-related response of the cortical bone to sham loading.

FE modeling predicted age altered load transmission within the bones

FE modeling predicted similar strains at the tibial medial mid-shaft to those measured by strain gauges. At the strain gauge location, the

Table 4
Endocortical and periosteal bone formation indices from mice subjected to axial tibial compression (left limb was dynamically loaded, right limb was nonloaded control) and mice subjected to sham loading (left limb was statically loaded with 1N, right limb was nonloaded control) (mean ± SD); for loaded mice groups: [a]within-subject effect of loading (loaded, control limbs), [b]between-subject effects of age (10 week old, 26 week old), and [c]interactions between these terms, $p < 0.05$ assessed using a repeated measures ANOVA.

	10 wk old				26 wk old			
	Loaded mice		Sham loaded mice		Loaded mice		Sham loaded mice	
Outcome	Loaded (n = 10)	Control (n = 10)	Sham loaded (n = 4)	Control (n = 4)	Loaded (n = 10)	Control (n = 10)	Sham loaded (n = 4)	Control (n = 4)
Ec.sLS/BS (%)[b]	10.9 ± 5.5	13.0 ± 9.5	15.5 ± 8.2	12.9 ± 6.9	21.0 ± 14.8	23.3 ± 7.3	20.6 ± 15.6	22.4 ± 16.4
Ec.dLS/BS (%)[a,b]	87.0 ± 6.2	80.4 ± 13.2	67.1 ± 15.6	83.3 ± 10.0	38.6 ± 13.8	15.4 ± 12.4	15.3 ± 11.3	20.5 ± 6.1
Ec.MS/BS (%)[a,b,c]	92.4 ± 4.3	86.9 ± 8.8	74.9 ± 12.2	89.8 ± 6.6	49.1 ± 7.7	27.1 ± 12.3	25.7 ± 11.9	31.7 ± 8.6
Ec.MAR (μm/day)[a,b]	2.08 ± 0.27	1.17 ± 0.34	1.33 ± 0.07	1.29 ± 0.13	1.64 ± 0.47	0.85 ± 0.35	0.55 ± 0.17	0.58 ± 0.21
Ec.BFR/BS (μm/day)[a,b,c]	1.92 ± 0.26	1.03 ± 0.36	1.00 ± 0.15	1.16 ± 0.16	0.81 ± 0.27	0.28 ± 0.18	0.15 ± 0.10	0.19 ± 0.11
Ps.sLS/BS (%)	26.9 ± 12.1	40.3 ± 26.5	30.8 ± 19.0	29.1 ± 17.0	23.7 ± 15.3	29.7 ± 27.1	21.6 ± 21.4	28.7 ± 11.3
Ps.dLS/BS (%)[a]	50.9 ± 16.6	10.0 ± 10.8	20.5 ± 12.6	17.6 ± 6.1	36.4 ± 19.6	12.1 ± 9.0	17.2 ± 13.5	15.0 ± 11.0
Ps.MS/BS (%)[a]	64.3 ± 13.4	30.2 ± 9.7	35.9 ± 7.5	32.2 ± 8.7	48.3 ± 19.8	26.9 ± 19.0	28.0 ± 14.9	29.3 ± 6.9
Ps.MAR (μm/day)[a,b,c]	1.67 ± 0.49	0.57 ± 0.15	0.90 ± 0.37	0.95 ± 0.60	1.03 ± 0.30	0.72 ± 0.17	0.41 ± 0.14	0.48 ± 0.20
Ps.BFR/BS (μm/day)[a,b,c]	1.09 ± 0.48	0.16 ± 0.05	0.32 ± 0.11	0.34 ± 0.28	0.53 ± 0.36	0.20 ± 0.15	0.13 ± 0.08	0.14 ± 0.05

FE model predicted strains of 1172 and 1121 με in the 10 and 26 wk bones. When predicting strains within the cortical bone, a VOI identical to that of the microCT analysis was used. For this cortical VOI, the FE model predicted similar strain distributions for the two different age groups, with the anterior side being under tension and the posterior under compression (Figs. 6C–D). The predicted strains were: average maximum principal strains (tensile) of 1174 με (standard deviation: 466) (10 week old) and 1080 με (standard deviation: 547) (26 week old) and average minimum principal strains (compressive) of −2410 με (standard deviation: 1660) (10 week old) and −1695 με (standard deviation: 1317) (26 week old). Lower average strains were predicted in the trabecular bone region: average maximum principal strains (tensile) of 867 με (standard deviation: 397) (10 week old) and 550 με (standard deviation: 157) (26 week old) and average minimum principal strains (compressive) of −1387 με (standard deviation: 900) (10 week old) and −915 με (standard deviation: 527) (26 week old). This VOI was similar to that used for microCT analysis of trabecular bone.

Effects of repeated radiation exposure on bone mass

When examining the effect of radiation exposure from microCT imaging, we observed that both the loaded and nonloaded control limbs from 10 week old mice that underwent multiple (0, 5, 10, 15 d) microCT scans (loaded limb, $n = 7$, 0.12 ± 0.01 mm^3/mm^3; control limb, $n = 7$, 0.05 ± 0.01 mm^3/mm^3) had significantly lower Tb.BV/TV compared to 10 week old mice that underwent only a single (15 d) microCT scan (loaded limb, $n = 4$, 0.15 ± 0.02 mm^3/mm^3; control limb, $n = 4$, 0.08 ± 0.01 mm^3/mm^3) ($p < 0.015$). Ten week old mice that underwent multiple (0, 5, 10, 15 d) microCT scans (loaded limb, $n = 7$, 322 ± 45 μm; control limb, $n = 7$, 356 ± 49 μm) also had significantly greater Tb.Sp compared to 10 week old mice that underwent only a single (15 d) microCT scan (loaded limb, $n = 4$, 249 ± 13 μm; control limb, $n = 4$, 257 ± 6 μm) ($p < 0.031$). No other microCT or histomorphometric parameters showed differences between the repeated radiated group compared to the single radiated group in the 10 week old mice and no differences were observed in any measured parameters for the 26 week old mice. A sub-analysis examining how aging influenced Tb.BV/TV, Tb.Sp only in the multiple radiated group ($n = 6$–7), still showed a significantly greater response to loading in the 10 week old mice compared to the 26 week old mice: BV/TV ($p < 0.001$), although the effect on Tb.Sp was slightly diminished ($p = 0.075$).

Discussion

Our aim was to investigate if mechanoresponsiveness is altered from youth to adulthood, with a focus on metaphyseal trabecular bone changes. We hypothesized that trabecular and cortical bone would respond anabolically to loading and that the bone response to mechanical loading would be reduced and the onset delayed in adult compared to postpubescent mice.

Although trabecular bone showed a robust anabolic response to loading in mice of both ages, the onset of an anabolic response to loading was observed earlier in young mice. Significant increases in bone volume fraction occurred already after 5 days in young mice, while the adult mice only showed a response after 10 days. Young mice showed significant thickening of trabeculae and increased bone mineral density in response to loading at day 10. Adult mice also showed a significant response to loading by steadily increasing trabecular thickness over the 15 days and preventing bone loss by maintaining bone volume fraction in the loaded limb at levels similar to those measured on day 0. In contrast, the nonloaded limb of these mice lost bone mass, showing a decreased BV/TV and trabecular thickness at day 15 compared to day 0. Mice at 26 weeks of age are fully grown and considered osteopenic in the proximal tibia, but are not yet senescent [76]. As has been reported for adult female C57Bl/6J mice [35], the nonloaded limb of adult mice and sham loaded adult mice showed a steady decrease in bone volume fraction and trabecular thickness as well as an increase in trabecular separation over the course of the experiment. These data are in contrast to those reported by Brodt et al. [60] and Silva et al. [77], who performed in vivo microCT and reported that loading decreased trabecular BV/TV in older male and female BALB/c mice. However, the loading waveform, duration of loading, and mouse strain were different from those used in our study and they did not perform FE modeling to estimate the level of strains transmitted to the trabeculae during loading. Therefore, it may be possible that the strain levels engendered in these mice did not reach osteogenic levels.

In agreement with our hypothesis, the trabecular bone of adult mice exhibited a reduced response to loading compared to the young mice by day 10, illustrated by trabecular bone volume fraction, architecture, and density. Our results are in accord with data from two previous studies which reported after two weeks of loading, a +49% and +95% (loaded versus control) increase in BV/TV from 26 week old and 10 week old female C57Bl/6J mice [24,26], while we observed a +50% and +117% (loaded versus control) increase in BV/TV, respectively. Interestingly our loading protocol required less than one fifth the number of loading cycles used in these studies to achieve a similar anabolic response in the trabecular bone. Previous studies have shown that a low number of cycles is adequate to elicit an anabolic response [78,79]. The addition of a five second rest insertion in our waveform may also have contributed to this observation, as these "rest" insertions have also been shown to enhance the anabolic response to loading in cortical bone [22]. In contrast, De Souza et al. [25] showed a +37%, −16.5%, and −37.5% (loaded versus control) change in BV/TV in 8, 12, and 20 week old female C57Bl/6J mice, respectively after two weeks of loading. They did not report the strain levels in the trabecular bone but used a greater load (−12 N) than the −11 N load we used here, which would be expected to generate greater cancellous strains. The loading waveform used by De Souza et al. [25] also included one tenth the number of loading cycles used in this study, 2 Hz rather than our 4 Hz cycle frequency, a 10 s rest compared to our 5 s rest, and a strain rate of approximately 1/10th (0.0015–0.002 ε/s) compared to 0.016 ε/s in the current study, which might explain the different trabecular responses to mechanical loading observed. A recent study [80] also showed no measureable trabecular adaptation to 5 and 7 N load levels, but did observe a 31% increase in trabecular BV/TV in 16 wk old female C57Bl/6 mice at 9 N, which shows the benefits of using multiple load levels within a study rather than choosing one peak value [63].

Surprisingly, there was no age-related difference between the 10 wk and 26 wk old mice in any trabecular histomorphometric parameters in response to loading. Since young and adult mice had similar Tb.MAR and Tb.MS/BS, the greater increase in BV/TV in the young mice in response to loading might be attributed to a decreased osteoclast response resulting in less bone resorbed in young mice, although this must be confirmed in future studies. Brodt et al. [60] also reported that loading enhanced dynamic trabecular histomorphometric measures, while microCT measures showed bone loss in 7 month old male BALB/c mice. They suggested that trabecular bone resorption was the reason for this apparent contradiction, although they were unable to detect an increase in osteoclast surface.

The young and adult mice had a similar onset in the response of cortical bone to loading with increases in cortical area and thickness apparent by day 10. At day 15, we measured a +13% and +9% (loaded versus control) increase in Ct.Ar and a +13% and +18% (loaded versus control) increase in Ct.Th in response to loading in young and adult mice, respectively. Lanyon's group [62,81] also reported positive increases in cortical bone after two weeks of loading: +16% and +24% (loaded versus control) in bone volume (mm^3) of 17 and 19 week old female C57Bl/6J mice, respectively. Silva's group [60]

also reported a modest increase of +11% (loaded versus control) in cortical bone volume (mm^3) after 5 days of loading in 7 month old BALB/c male mice and a +3% and +6% increase (loaded versus control) in cortical bone volume (mm^3) after three weeks of loading (3 days/week) in 2 and 4 month old BALB/c female mice, respectively [77]. A more pronounced response of +48% and +40% (loaded versus control) increase in cortical area (mm^2) of 10 and 26 week [26] old female C57Bl/6J mice was shown after two weeks of loading at similar load levels (11 N). However, the loading protocol used in the said study included more cycles of loading and a higher reported strain engendered in the 26 week old mice (2300 με, strain gauge value) than that used in this study, which may explain the more pronounced cortical response compared to our results. In our study all cortical bone formation indices measured at day 15, except those associated with single labeled surface, were enhanced by loading in young and adult mice, with a greater absolute value in all parameters in the young compared to adult mice.

In contrast to our hypothesis, microCT parameters and most histmorphometric bone formation indices indicated no reduction in mechanoresponsiveness of cortical bone between young and adult mice. After two weeks of loading, we observed a +78% and +93% (loaded versus control) increase in Ec.MAR and a +86% and +189% (loaded versus control) increase in Ec. BFR/BS in 10 week old and 26 week old female C57Bl/6J mice, respectively. Additionally, we observed a +193% and +43% (loaded versus control) increase in Ps.MAR and a +581% and +165% (loaded versus control) increase in Ps.BFR/BS in 10 week old and 26 week old female C57Bl/6J mice, respectively. These data suggest that although the overall response to loading was similar for the different aged mice, as seen in the microCT parameters, there seemed to be an age-specific regional response to loading with a greater response periosteally in young mice and endosteally in the adult mice. Lynch et al. [24,26] reported that greater periosteal expansion in young mice compared to adult mice was due to a greater periosteal perimeter in adult mice, which would require a smaller increase in cortical thickness by periosteal bone deposition to increase bending resistance to a similar degree as in young mice. The young mice are not skeletally mature and thus the anabolic response to loading against the background of growth or a more quiescent state must be considered [82]. However, our data also showed a similar trabecular MAR, Ps.MAR, and Ps.BFR/BS for the nonloaded limb of both ages. Although, Ec.MAR and Ec.BFR/BS of the nonloaded limb was lower in the 26 week olds compared to the 10 week olds, suggesting minor growth differences.

We observed an effect of radiation exposure from microCT imaging on the Tb.BV/TV and Tb.Sp of 10 week old mice. However, the observed effect of radiation +25% (single scanned loaded limb versus multiple scanned loaded limb) was much less than the observed increase in trabecular BV/TV due to loading +117% (loaded limb versus control limb for combined group $n = 11$). Interestingly, the increase in trabecular BV/TV due to loading was higher in the multiple scanned group +140% (loaded limb versus control limb, $n = 7$) compared to the single scanned group +88% (loaded limb versus control limb, $n = 4$). This suggests that radiation does not hamper the bone's response to mechanical load. This outcome has important ramifications in regard to astronauts during space flight, who are exposed to both solar and cosmic radiation [83] as well as to cancer patients undergoing radiation therapy. However, the cellular and molecular mechanisms behind this outcome remain unknown. Also, it is unclear why we observed radiation effects only in young growing mice and not skeletally mature mice. Klinck et al. [84] previously reported that mouse strains such as C57Bl/6 are more sensitive to radiation effects because they have comparatively lower bone volume fraction than other strains, but this would not explain why 10 wk old mice, who have greater Tb.BV/TV compared to 26 wk old mice, would be affected by radiation. These questions require further study. Additionally, because we do not have baseline parameters at day 0 for the single scanned group, we do not know how these parameters changed over time and whether the differences observed were due to radiation or initial variation between animals. However, Klinck et al. [84] reported baseline data and observed similar small, but statistically significant decreases in trabecular BV/TV from the proximal tibia of 12 week old female C57Bl/6J mice that underwent five weekly scans compared to unscanned limbs. In contrast, Buie et al. [85] reported no differences in trabecular BV/TV from the proximal tibia of 6 week old female C57Bl/6J mice that underwent 12 scans compared to 6 scans on a weekly basis. Future studies performing repeated in vivo microCT analyses should consider these effects, especially when examining skeletally immature mice.

Our tibial strain distribution maps are comparable to those reported by others [72,86]. Strain levels were highest at the mid-diaphysis where bending of the bone was predicted. Finite element models predicted a lower average mechanical strain in both, the cortical and trabecular regions, in adult compared to young mice. The average mechanical strain induced in cortical and trabecular regions in the 26 wk mice were 18% and 32% lower than in the 10 wk old mice, respectively. These results are contrary to previous finite element studies showing that, under the same externally applied load, there was increased mechanical strain in 26 week old compared to 10 week old mice in the cortical region, while no significant differences were found in the trabecular region [27].

Previous studies have ignored alterations in bone tissue material properties which occur with aging [58,59], as well as the highly heterogeneous nature of the bone [87]. When the 10 and 26 wk old bones were considered to have the same homogeneous Young modulus (15GPa), the induced strains in cortical and trabecular regions were on average 20% and 5% higher in the 26 wk old mice compared to the 10 wk old mice, while at the strain gauge site the average strains were 690 and 903 με for 10 and 26 wk old mice. It is known that with age there is an increase in the elasticity of the bone. Somerville et al. [59] measured a 10% increase in tissue elasticity from 10 to 26 wk in C57Bl/6J mice. The increase in bone elastic modulus [59] and cross-sectional moment of inertia (Table 4) with age would result in a decreased strain in the older mice for a given force, which we did not observe at the medial midshaft. However, this apparent contradiction can be explained by changes in whole bone geometry with aging. The bones of 26 wk old mice are more curved than those of 10 wk old mice [26,64] which will increase their bending stresses under a given load and counteract age-related increases in mineral and geometric properties. Our FE models predicted approximately 1200 με at the strain gauge position on the medial midshaft of the tibia. However, when we analyzed different positions within the bone, the FE models predicted lower strains at the same load in 26 week old mice compared to 10 wk old mice, suggesting that strain gauging one position is inadequate to characterize the strain distribution.

In this study, we have incorporated not only age-related alterations in bone material properties, but also, to some extent, regional differences in the elasticity of the bone (fibula, proximal and distal). We have seen that these alterations play a key role in the induced bone tissue strains. Although, we are aware that bone material properties are more complex that what we have implemented in our models (e.g. anisotropy), we have been able to show that with age there is a change in the way the load is transmitted within the bone and that this is due to both, alterations in the geometry of the bone and in its tissue material properties. Our reduced response of the trabecular bone to loading with age coincides with lower induced strains in this region. However, in the cortical region we observed no differences in the bone response with age while lower strains were predicted in the older animals. Further studies should aim to understand whether local bone formation/resorption sites occur in regions under significantly different levels of mechanical strain in both age groups.

Some controversy exists over the presence of systemic effects of unilateral mechanical loading in rodents [88,89] after Sample et al. [90]

showed noninvasive mechanical loading of the radius and ulna in young rats stimulated regional (re)modeling responses within the limb beyond the loaded bones and systemic (re)modeling effects in the bones of the contralateral limb that may be mediated by the nervous system. Data from nonloaded contralateral limbs in our study showed no apparent response to loading. While the bone volume fraction of the nonloaded limb of the young mice remained relatively constant, the nonloaded limb of adult mice and sham loaded adult mice showed a steady decrease in bone volume fraction and trabecular thickness as well as an increase in trabecular separation over the course of the experiment [35]. Our data supports the findings of Sugiyama et al. [81] showing that functional adaptation in both cortical and trabecular bone was controlled locally and confined to the loaded bone.

The tibial loading model used in our study [24–26,61] has major benefits over previously published mouse ulnar loading models [91] in that the adaptive response to mechanical loading of trabecular bone as well as cortical bone can be analyzed simultaneously using a noninvasive approach, as the tibia has more trabecular bone than the ulna. It could be argued that trabecular bone is more clinically relevant to examine in the context of its response to mechanical loading than cortical bone due to its involvement in diseases such as osteoporosis or osteoarthritis related-total joint replacement. A strength of our study was the longitudinal assessment of cortical and trabecular bone, which allowed us to better understand and interpret how these tissues respond to mechanical loading over time. It is important to understand the kinetics of bone gain after mechanical loading as exercise may be used to augment drug therapies targeting either anabolic or catabolic processes. Also, our two week loading protocol allowed sufficient time to observe changes, especially in trabecular bone, that would have been missed with a shorter loading duration, such as one week [60]. The inclusion of sham loaded mice reinforced the local nature of the response to loading and emphasized the consistency in our data when comparing the response in sham-loaded limbs to the nonloaded right limb of the loaded mice. Lastly, our in vivo strain gauging and FE modeling, which are largely absent in many published loading studies, allowed us to better estimate strains and thereby compare the mechanoresponsiveness in different aged mice.

In summary, our data indicated that two weeks of loading elicited a strong anabolic response in both trabecular and cortical bone of 10 and 26 week old female C57Bl/6J mice. In agreement with our hypothesis, the trabecular bone of adult mice exhibited a reduced and delayed response to loading compared to the young female C57Bl/6J mice, apparent in trabecular bone volume fraction and architecture by day 10. We saw no loss in short-term mechanosensitivity in the cortical bone between the young and adult mice. In terms of the mechanics of the bone, we saw an age-related reduction in the induced deformation of the bone under the same externally applied load. Together these data suggest that trabecular bone loss that occurs in adulthood may not be only due to a reduced mechanoresponsiveness in this tissue, but also that alterations in the load induced strains within the bone may play a key role.

Acknowledgments

This study was partially supported by the German Federal Ministry of Education and Research (Bundesministerium für Bildung und Forschung; Osteopath grant/TP6) and the German Research Foundation (Deutsche Forschungsgemeinschaft; WI 3761/1-1).

Authors' roles: Obtained funding: BMW, GND. Study design: BMW, GND. Data acquisition: AB, TT, MA, BK, HR, AS, RPM, BMW. Data analysis: BMW. Data interpretation: BMW, GND, SC, RPM. Drafting manuscript: BMW. Revising manuscript content: All authors. Approving final version of manuscript: All authors. BMW takes responsibility for the integrity of the data.

Conflict of interest

All authors state that they have no conflicts of interest.

References

[1] Jones HH, Priest JD, Hayes WC, Tichenor CC, Nagel DA. Humeral hypertrophy in response to exercise. J Bone Joint Surg Am 1977;59:204–8.
[2] Haapasalo H, Kontulainen S, Sievanen H, Kannus P, Jarvinen M, Vuori I. Exercise-induced bone gain is due to enlargement in bone size without a change in volumetric bone density: a peripheral quantitative computed tomography study of the upper arms of male tennis players. Bone 2000;27:351–7.
[3] Kontulainen S, Sievanen H, Kannus P, Pasanen M, Vuori I. Effect of long-term impact-loading on mass, size, and estimated strength of humerus and radius of female racquet-sports players: a peripheral quantitative computed tomography study between young and old starters and controls. J Bone Miner Res 2003;18:352–9.
[4] Wittich A, Mautalen CA, Oliveri MB, Bagur A, Somoza F, Rotemberg E. Professional football (soccer) players have a markedly greater skeletal mineral content, density and size than age- and BMI-matched controls. Calcif Tissue Int 1998;63:112–7.
[5] Fuchs RK, Bauer JJ, Snow CM. Jumping improves hip and lumbar spine bone mass in prepubescent children: a randomized controlled trial. J Bone Miner Res 2001;16:148–56.
[6] Heinonen A, Kannus P, Sievanen H, Oja P, Pasanen M, Rinne M, et al. Randomised controlled trial of effect of high-impact exercise on selected risk factors for osteoporotic fractures. Lancet 1996;348:1343–7.
[7] Kato T, Terashima T, Yamashita T, Hatanaka Y, Honda A, Umemura Y. Effect of low-repetition jump training on bone mineral density in young women. J Appl Physiol 2006;100:839–43.
[8] Vainionpaa A, Korpelainen R, Leppaluoto J, Jamsa T. Effects of high-impact exercise on bone mineral density: a randomized controlled trial in premenopausal women. Osteoporos Int 2005;16:191–7.
[9] Vainionpaa A, Korpelainen R, Vihriala E, Rinta-Paavola A, Leppaluoto J, Jamsa T. Intensity of exercise is associated with bone density change in premenopausal women. Osteoporos Int 2006;17:455–63.
[10] Kerr D, Morton A, Dick I, Prince R. Exercise effects on bone mass in postmenopausal women are site-specific and load-dependent. J Bone Miner Res 1996;11:218–25.
[11] Kohrt WM, Ehsani AA, Birge Jr SJ. Effects of exercise involving predominantly either joint-reaction or ground-reaction forces on bone mineral density in older women. J Bone Miner Res 1997;12:1253–61.
[12] Kohrt WM, Snead DB, Slatopolsky E, Birge Jr SJ. Additive effects of weight-bearing exercise and estrogen on bone mineral density in older women. J Bone Miner Res 1995;10:1303–11.
[13] Bassey EJ, Rothwell MC, Littlewood JJ, Pye DW. Pre- and postmenopausal women have different bone mineral density responses to the same high-impact exercise. J Bone Miner Res 1998;13:1805–13.
[14] Hoshi A, Watanabe H, Chiba M, Inaba Y. Effects of exercise at different ages on bone density and mechanical properties of femoral bone of aged mice. Tohoku J Exp Med 1998;185:15–24.
[15] Silbermann M, Bar-Shira-Maymon B, Coleman R, Reznick A, Weisman Y, Steinhagen-Thiessen E, et al. Long-term physical exercise retards trabecular bone loss in lumbar vertebrae of aging female mice. Calcif Tissue Int 1990;46:80–93.
[16] Jarvinen TL, Pajamaki I, Sievanen H, Vuohelainen T, Tuukkanen J, Jarvinen M, et al. Femoral neck response to exercise and subsequent deconditioning in young and adult rats. J Bone Miner Res 2003;18:1292–9.
[17] Raab DM, Smith EL, Crenshaw TD, Thomas DP. Bone mechanical properties after exercise training in young and old rats. J Appl Physiol 1990;68:130–4.
[18] Umemura Y, Ishiko T, Tsujimoto H, Miura H, Mokushi N, Suzuki H. Effects of jump training on bone hypertrophy in young and old rats. Int J Sports Med 1995;16:364–7.
[19] Buhl KM, Jacobs CR, Turner RT, Evans GL, Farrell PA, Donahue HJ. Aged bone displays an increased responsiveness to low-intensity resistance exercise. J Appl Physiol 2001;90:1359–64.
[20] Leppanen OV, Sievanen H, Jokihaara J, Pajamaki I, Kannus P, Jarvinen TL. Pathogenesis of age-related osteoporosis: impaired mechano-responsiveness of bone is not the culprit. PLoS One 2008;3:e2540.
[21] Rubin CT, Bain SD, McLeod KJ. Suppression of the osteogenic response in the aging skeleton. Calcif Tissue Int 1992;50:306–13.
[22] Srinivasan S, Agans SC, King KA, Moy NY, Poliachik SL, Gross TS. Enabling bone formation in the aged skeleton via rest-inserted mechanical loading. Bone 2003;33:946–55.
[23] Turner CH, Takano Y, Owan I. Aging changes mechanical loading thresholds for bone formation in rats. J Bone Miner Res 1995;10:1544–9.
[24] Lynch ME, Main RP, Xu Q, Walsh DJ, Schaffler MB, Wright TM, et al. Cancellous bone adaptation to tibial compression is not sex dependent in growing mice. J Appl Physiol 2010;109:685–91.
[25] De Souza RL, Matsuura M, Eckstein F, Rawlinson SC, Lanyon LE, Pitsillides AA. Non-invasive axial loading of mouse tibiae increases cortical bone formation and modifies trabecular organization: a new model to study cortical and cancellous compartments in a single loaded element. Bone 2005;37:810–8.
[26] Lynch ME, Main RP, Xu Q, Schmicker TL, Schaffler MB, Wright TM, et al. Tibial compression is anabolic in the adult mouse skeleton despite reduced responsiveness with aging. Bone 2011;49:439–46.
[27] Rizzoli R, Bonjour JP, Ferrari SL. Osteoporosis, genetics and hormones. J Mol Endocrinol 2001;26:79–94.
[28] Seeman E, Delmas PD. Bone quality — the material and structural basis of bone strength and fragility. N Engl J Med 2006;354:2250–61.
[29] Croucher PI, Garrahan NJ, Mellish RW, Compston JE. Age-related changes in resorption cavity characteristics in human trabecular bone. Osteoporos Int 1991;1:257–61.

[30] Eriksen EF, Langdahl B, Vesterby A, Rungby J, Kassem M. Hormone replacement therapy prevents osteoclastic hyperactivity: A histomorphometric study in early postmenopausal women. J Bone Miner Res 1999;14:1217–21.
[31] Riggs BL, Melton LJ, Robb RA, Camp JJ, Atkinson EJ, McDaniel L, et al. A population-based assessment of rates of bone loss at multiple skeletal sites: evidence for substantial trabecular bone loss in young adult women and men. J Bone Miner Res 2008;23:205–14.
[32] Riggs BL, Wahner HW, Melton III LJ, Richelson LS, Judd HL, Offord KP. Rates of bone loss in the appendicular and axial skeletons of women. Evidence of substantial vertebral bone loss before menopause. J Clin Invest 1986;77:1487–91.
[33] Gilsanz V, Gibbens DT, Carlson M, Boechat MI, Cann CE, Schulz EE. Peak trabecular vertebral density: a comparison of adolescent and adult females. Calcif Tissue Int 1988;43:260–2.
[34] Seeman E. Modeling and Remodeling: The cellular machinery responsible for the gain and loss of bone's material and structural strength. In: Bilezikian John P, editor. Principles of bone biology. 3rd ed. New York: Academic Press; 2008. p. 3–28.
[35] Glatt V, Canalis E, Stadmeyer L, Bouxsein ML. Age-related changes in trabecular architecture differ in female and male C57BL/6J mice. J Bone Miner Res 2007;22: 1197–207.
[36] Carmona RH. Surgeon general reports on bone health. J Calif Dent Assoc Jan 2005;33: 9–11.
[37] Melton III LJ, Riggs BL, Achenbach SJ, Amin S, Camp JJ, Rouleau PA, et al. Does reduced skeletal loading account for age-related bone loss? J Bone Miner Res 2006;21:1847–55.
[38] Lanyon L, Skerry T. Postmenopausal osteoporosis as a failure of bone's adaptation to functional loading: a hypothesis. J Bone Miner Res 2001;16:1937–47.
[39] Aloia JF, McGowan DM, Vaswani AN, Ross P, Cohn SH. Relationship of menopause to skeletal and muscle mass. Am J Clin Nutr 1991;53:1378–83.
[40] Kallman DA, Plato CC, Tobin JD. The role of muscle loss in the age-related decline of grip strength: cross-sectional and longitudinal perspectives. J Gerontol 1990;45:M82–8.
[41] Burr DB. Muscle strength, bone mass, and age-related bone loss. J Bone Miner Res 1997;12:1547–51.
[42] Akkus O, Adar F, Schaffler MB. Age-related changes in physicochemical properties of mineral crystals are related to impaired mechanical function of cortical bone. Bone 2004;34:443–53.
[43] Nordin BE, Need AG, Chatterton BE, Horowitz M, Morris HA. The relative contributions of age and years since menopause to postmenopausal bone loss. J Clin Endocrinol Metab 1990;70:83–8.
[44] Slemenda C, Hui SL, Longcope C, Johnston CC. Sex steroids and bone mass. A study of changes about the time of menopause. J Clin Invest 1987;80:1261–9.
[45] Villareal DT, Morley JE. Trophic factors in aging. Should older people receive hormonal replacement therapy? Drugs Aging 1994;4:492–509.
[46] Frost HM. On the estrogen–bone relationship and postmenopausal bone loss: a new model. J Bone Miner Res 1999;14:1473–7.
[47] Lee K, Jessop H, Suswillo R, Zaman G, Lanyon L. Endocrinology: bone adaptation requires oestrogen receptor-alpha. Nature 2003;424:389.
[48] Sahin E, Depinho RA. Linking functional decline of telomeres, mitochondria and stem cells during ageing. Nature 2010;464:520–8.
[49] Fedarko NS, Vetter UK, Robey PG. Age-related changes in bone matrix structure in vitro. Calcif Tissue Int 1995;56(Suppl. 1):S41–3.
[50] Stanford CM, Welsch F, Kastner N, Thomas G, Zaharias R, Holtman K, et al. Primary human bone cultures from older patients do not respond at continuum levels of in vivo strain magnitudes. J Biomech 2000;33:63–71.
[51] Klein-Nulend J, Sterck JG, Semeins CM, Lips P, Joldersma M, Baart JA, et al. Donor age and mechanosensitivity of human bone cells. Osteoporos Int 2002;13:137–46.
[52] Sterck JG, Klein-Nulend J, Lips P, Burger EH. Response of normal and osteoporotic human bone cells to mechanical stress in vitro. Am J Physiol 1998;274:E1113–20.
[53] Termine JD. Cellular activity, matrix proteins, and aging bone. Exp Gerontol 1990;25:217–21.
[54] Kita K, Kawai K, Hirohata K. Changes in bone marrow blood flow with aging. J Orthop Res 1987;5:569–75.
[55] Tonna EA. Electron microscopic study of bone surface changes during aging. The loss of cellular control and biofeedback. J Gerontol 1978;33:163–77.
[56] Ehrlich PJ, Lanyon LE. Mechanical strain and bone cell function: a review. Osteoporos Int 2002;13:688–700.
[57] Nicolella DP, Yao W, Lane N. Estrogen deficiency alters the localized material properties of the peri-lacunar bone matrix in old rats. J Bone Miner Res 2008;23(Suppl. 1).
[58] Brodt MD, Ellis CB, Silva MJ. Growing C57Bl/6 mice increase whole bone mechanical properties by increasing geometric and material properties. J Bone Miner Res 1999;14:2159–66.
[59] Somerville JM, Aspden RM, Armour KE, Armour KJ, Reid DM. Growth of C57BL/6 mice and the material and mechanical properties of cortical bone from the tibia. Calcif Tissue Int 2004;74:469–75.
[60] Brodt MD, Silva MJ. Aged mice have enhanced endocortical response and normal periosteal response compared with young-adult mice following 1 week of axial tibial compression. J Bone Miner Res 2010;25:2006–15.
[61] Fritton JC, Myers ER, Wright TM, van der Meulen MC. Loading induces site-specific increases in mineral content assessed by microcomputed tomography of the mouse tibia. Bone 2005;36:1030–8.
[62] Sugiyama T, Saxon LK, Zaman G, Moustafa A, Sunters A, Price JS, et al. Mechanical loading enhances the anabolic effects of intermittent parathyroid hormone (1–34) on trabecular and cortical bone in mice. Bone 2008;43:238–48.
[63] Sugiyama T, Meakin LB, Browne WJ, Galea GL, Price JS, Lanyon LE. Bones' adaptive response to mechanical loading is essentially linear between the low strains associated with disuse and the high strains associated with the lamellar/woven bone transition. J Bone Miner Res 2012;27:1784–93.
[64] Main RP, Lynch ME, van der Meulen MC. In vivo tibial stiffness is maintained by whole bone morphology and cross-sectional geometry in growing female mice. J Biomech 2010;43:2689–94.
[65] Biewener AA. In vivo measurement of bone strain and tendon force. In: Biewener AA, editor. Biomechanics — structures and systems: a practical approach. Oxford University Press; 1992. p. 123–41.
[66] Clarke KA, Still J. Gait analysis in the mouse. Physiol Behav 1999;66:723–9.
[67] Turner CH, Owan I, Takano Y. Mechanotransduction in bone: role of strain rate. Am J Physiol 1995;269:E438–42.
[68] Mosley JR, Lanyon LE. Strain rate as a controlling influence on adaptive modeling in response to dynamic loading of the ulna in growing male rats. Bone 1998;23:313–8.
[69] Bouxsein ML, Boyd SK, Christiansen BA, Guldberg RE, Jepsen KJ, Muller R. Guidelines for assessment of bone microstructure in rodents using micro-computed tomography. J Bone Miner Res 2010;25:1468–86.
[70] Parfitt AM, Drezner MK, Glorieux FH, Kanis JA, Malluche H, Meunier PJ, et al. Bone histomorphometry: standardization of nomenclature, symbols, and units. Report of the ASBMR Histomorphometry Nomenclature Committee. J Bone Miner Res 1987;2:595–610.
[71] Foldes J, Shih MS, Parfitt AM. Frequency distributions of tetracycline-based measurements: implications for the interpretation of bone formation indices in the absence of double-labeled surfaces. J Bone Miner Res 1990;5:1063–7.
[72] Stadelmann VA, Hocke J, Verhelle J, Forster V, Merlini F, Terrier A, et al. 3D strain map of axially loaded mouse tibia: a numerical analysis validated by experimental measurements. Comput Methods Biomech Biomed Engin 2009;12:95–100.
[73] Taddei F, Schileo E, Helgason B, Cristofolini L, Viceconti M. The material mapping strategy influences the accuracy of CT-based finite element models of bones: an evaluation against experimental measurements. Med Eng Phys 2007;29:973–9.
[74] Schileo E, Taddei F, Malandrino A, Cristofolini L, Viceconti M. Subject-specific finite element models can accurately predict strain levels in long bones. J Biomech 2007;40:2982–9.
[75] Carter DR, Hayes WC. The compressive behavior of bone as a two-phase porous structure. J Bone Joint Surg Am 1977;59:954–62.
[76] Flurkey K, Currer J, Harrison D. Mouse models in aging research. In: Fox J, editor. The mouse in biomedical research. 2nd ed. Burlington, MA: American College Laboratory Animal Medicine (Elsevier); 2007. p. 637–72.
[77] Silva MJ, Brodt MD, Lynch MA, Stephens AL, Wood DJ, Civitelli R. Tibial loading increases osteogenic gene expression and cortical bone volume in mature and middle-aged mice. PLoS One 2012;7:e34980.
[78] Rubin CT, Lanyon LE. Regulation of bone formation by applied dynamic loads. J Bone Joint Surg Am 1984;66:397–402.
[79] Robling AG, Burr DB, Turner CH. Partitioning a daily mechanical stimulus into discrete loading bouts improves the osteogenic response to loading. J Bone Miner Res 2000;15:1596–602.
[80] Weatherholt AM, Fuchs RK, Warden SJ. Cortical and trabecular bone adaptation to incremental load magnitudes using the mouse tibial axial compression loading model. Bone 2013;52:372–9.
[81] Sugiyama T, Price JS, Lanyon LE. Functional adaptation to mechanical loading in both cortical and cancellous bone is controlled locally and is confined to the loaded bones. Bone 2010;46:314–21.
[82] Mosley JR, Lanyon LE. Growth rate rather than gender determines the size of the adaptive response of the growing skeleton to mechanical strain. Bone 2002;30:314–9.
[83] Lloyd SA, Bandstra ER, Willey JS, Riffle SE, Tirado-Lee L, Nelson GA, et al. Effect of proton irradiation followed by hindlimb unloading on bone in mature mice: a model of long-duration spaceflight. Bone 2012;51:756–64.
[84] Klinck RJ, Campbell GM, Boyd SK. Radiation effects on bone architecture in mice and rats resulting from in vivo micro-computed tomography scanning. Med Eng Phys 2008;30:888–95.
[85] Buie HR, Moore CP, Boyd SK. Postpubertal architectural developmental patterns differ between the L3 vertebra and proximal tibia in three inbred strains of mice. J Bone Miner Res 2008;23:2048–59.
[86] Moustafa A, Sugiyama T, Prasad J, Zaman G, Gross TS, Lanyon LE, et al. Mechanical loading-related changes in osteocyte sclerostin expression in mice are more closely associated with the subsequent osteogenic response than the peak strains engendered. Osteoporos Int 2012;23:1225–34.
[87] Cattaneo PM, Dalstra M, Frich LH. A three-dimensional finite element model from computed tomography data: a semi-automated method. Proc Inst Mech Eng H 2001;215:203–13.
[88] Rubin J, Rubin C. Functional adaptation to loading of a single bone is neuronally regulated and involves multiple bones. J Bone Miner Res 2008;23:1369–71.
[89] Skerry TM, Lanyon LE. Systemic and contralateral responses to loading of bones. J Bone Miner Res 2009;24:753 [author reply 754].
[90] Sample SJ, Behan M, Smith L, Oldenhoff WE, Markel MD, Kalscheur VL, et al. Functional adaptation to loading of a single bone is neuronally regulated and involves multiple bones. J Bone Miner Res 2008;23:1372–81.
[91] Lee KC, Maxwell A, Lanyon LE. Validation of a technique for studying functional adaptation of the mouse ulna in response to mechanical loading. Bone 2002;31:407–12.
[92] Birkhold A, Checa S, Duda GN, Willie BM. Global and site-specific adaptation of cancellous bone to in vivo loading. 18th Congress of the European Society of Biomechanics; 2012. p. 01291.